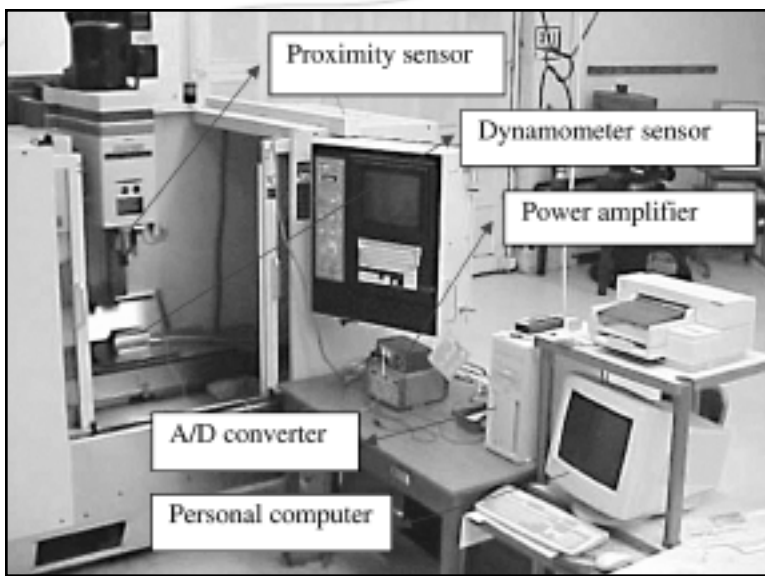


Figure 1. Experimental setup for the proposed MLR-IPSRR system.



The hardware included:

- A Fadal vertical CNC milling machine with multiple tool changing and a 15 HP spindle.
- A Kistler 9257B type dynamometer sensor, which provided dynamic measurement of the three orthogonal components of a force signal (F_x , F_y , and F_z).
- A Micro Switch 922 series 3-wire DC proximity sensor, used to collect the signal for counting the rotations of the spindle as the tool was cutting.
- A power supplier, used to amplify the signals from the proximity and the dynamometer sensors. This amplified signal was then sent to the A/D board.
- An omega CIO-DAS-1602/12 A/D converter, used to convert both the dynamometer and proximity sensor data from analog to digital signals.
- A P5 133 personal computer, which was connected to collect data from the A/D converter output via an I/O interface.

- A 6061 aluminum workpiece with dimensions of 1.00" x 1.00" x 1.00", which was cut in the end milling operations.

In order to control end milling operations and analyze the spindle revolution and cutting force signals, the following software was required: (a) Basic CNC codes, which were applied to conduct cutting operations, and (b) A/D converter software, which was used to convert data (proximity and cutting forces) from analog signals to digital values. Using the hardware and software setups, tests of cut were performed. Figure 2 shows the data obtained from this experimental run using spindle speed ($S = 2500$ rpm), feed rate ($F = 8$ ipm), and depth of cut ($D = 0.08$ in.).

The Cutting Forces Analysis

From Figure 2, the cutting force data were collected from the dynamometer sensor; these three forces (F_x , F_y , and F_z) cannot individually represent the actual force affecting surface rough-

**Figure 2. Proximity and cutting force digital data using cutting condition
 $S = 2500$ rpm, $F = 8$ ipm, and $D = 0.08$ in.**

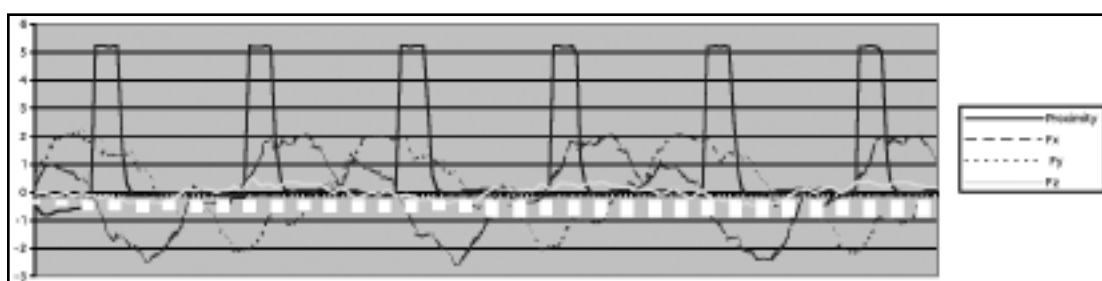
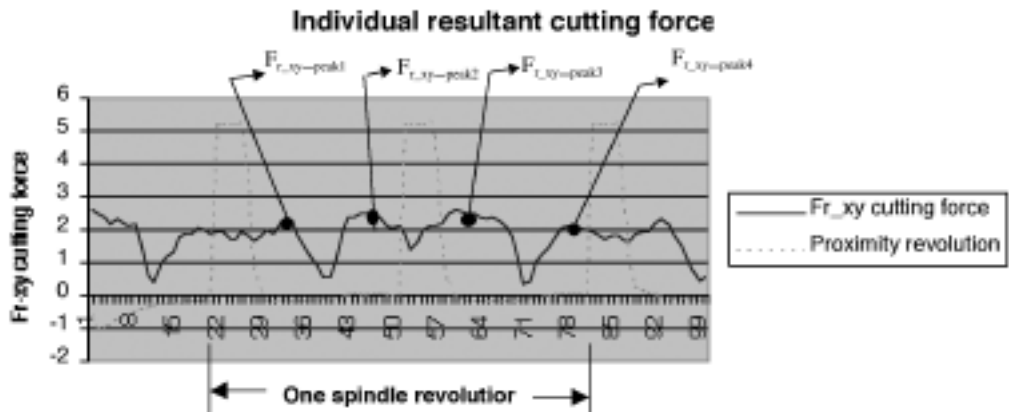


Figure 3. Individual resultant cutting force F_{r_xy} and four peak forces in one revolution at cutting condition of $F = 20$ ipm, $S = 2000$ rpm, $D = 0.08$ in.



ness. Four cutting force magnitudes (\bar{F}_{r_xy} , $\bar{F}_{r_xy_peak}$, \bar{F}_z , and \bar{F}_{r_xyz}) were considered as possible candidates for an input factor for the MLR-IPSRR system. They are defined as:

1. Average resultant force of the x and y directions per revolution (\bar{F}_{r_xy}).

By using the following equation, one could find the individual resultant force (F_{r_xy}) from the x and y directions as shown in Figure 3.

$$\bar{F}_{r_xy,i} = \sqrt{F_{x,i}^2 + F_{y,i}^2}, \quad (1)$$

where i is the data point in one revolution. Then, the average resultant force in one revolution (\bar{F}_{r_xy}) could be given as:

$$\bar{F}_{r_xy} = \frac{\sum_{i=1}^m \bar{F}_{r_xy,i}}{m}, \quad (2)$$

where $i = 1, 2, \dots, m$ and m is the total data points in one revolution.

2. Average resultant peak force ($\bar{F}_{r_xy_peak}$).

By using the data shown in Figure 3, one could also identify the peak force ($F_{r_xy_peak}$) from the average resultant forces of the x and y directions (\bar{F}_{r_xy}) in the cut period of each tooth. Then, the average resultant peak force in each revolution ($\bar{F}_{r_xy_peak}$) could be given as:

$$\bar{F}_{r_xy_peak} = \frac{\sum_{i=1}^r F_{r_xy_peak,i}}{r}, \quad (3)$$

where $i = 1, 2, \dots, r$ and r is the number of cut-

ting tool teeth. In this study, $r = 4$.

3. Average z direction cutting force per revolution (\bar{F}_z).

The third type of force analyzed in this study was the average cutting force in the z direction per revolution (\bar{F}_z) and could be given as:

$$\bar{F}_z = \frac{\sum_{i=1}^m F_{z,i}}{m}, \quad (4)$$

where $i = 1, 2, \dots, m$ and m is the total data points in one revolution.

4. Average resultant force of x, y, and z directions per revolution (\bar{F}_{r_xyz}).

The researcher also wanted to analyze the average resultant force of the x, y, and z directions in one revolution (\bar{F}_{r_xyz}). The force is given as:

$$\bar{F}_{r_xyz,i} = \sqrt{F_{x,i}^2 + F_{y,i}^2 + F_{z,i}^2}, \quad (5)$$

where i is the data point in one revolution. Then, the average resultant force in one revolution (\bar{F}_{r_xyz}) could be given as:

$$\bar{F}_{r_xyz} = \frac{\sum_{i=1}^m \bar{F}_{r_xyz,i}}{m}, \quad (6)$$

where $i = 1, 2, 3, \dots, m$ and m is the total data points in one revolution.

After the above-mentioned cutting forces were formed, we examined the correlation coefficient between these cutting forces and surface roughness. Equation 7 was used to compute the

correlation coefficient between surface roughness (R_a) and the average resultant force of the x and y directions ($\bar{F}_{r_{xy}}$).

$$\rho_{Ra-\bar{F}_{r_{xy}}} = \frac{\sum_{i=1}^n (Ra_i - \bar{R}_a)(\bar{F}_{r_{xy}}_i - \bar{\bar{F}}_{r_{xy}})}{\sqrt{\sum_{i=1}^n (Ra_i - \bar{R}_a)^2} \sqrt{\sum_{i=1}^n (\bar{F}_{r_{xy}}_i - \bar{\bar{F}}_{r_{xy}})^2}}, \quad (7)$$

where ρ is the correlation coefficient between the average resultant cutting force ($\rho_{Ra-\bar{F}_{r_{xy}}}$) and surface roughness, Rai is the i th surface roughness, $i = 1, 2, \dots, n$ (n is total data sets; here $n = 384$), and $\bar{F}_{r_{xy}}$ is the i th average resultant cutting force of the x and y directions, $i = 1, 2, \dots, n$, (n is total data sets; here $n = 384$).

$$\bar{R}_a = \frac{\sum_{i=1}^n Ra_i}{n}, \quad \bar{F}_{r_{xy}} = \frac{\sum_{i=1}^n \bar{F}_{r_{xy}}_i}{n}$$

Similarly, the \bar{F}_{r_z} and $\bar{F}_{r_{xyz}}$ were calculated. The largest value of correlation coefficients between the above-mentioned cutting forces and surface roughness represented the most significant cutting force, which was then used in the development of the MLR-IPSRR system.

Experimental Design

In order to identify the most significant cutting force for the MLR-IPSRR system, an experimental design matrix was used to run and collect the training data. The experimental design matrix, including eight levels of feed rate (6, 8, 10, 12, 14, 16, 18, and 20 ipm), four levels of spindle speed (1750, 2000, 2250, and 2500

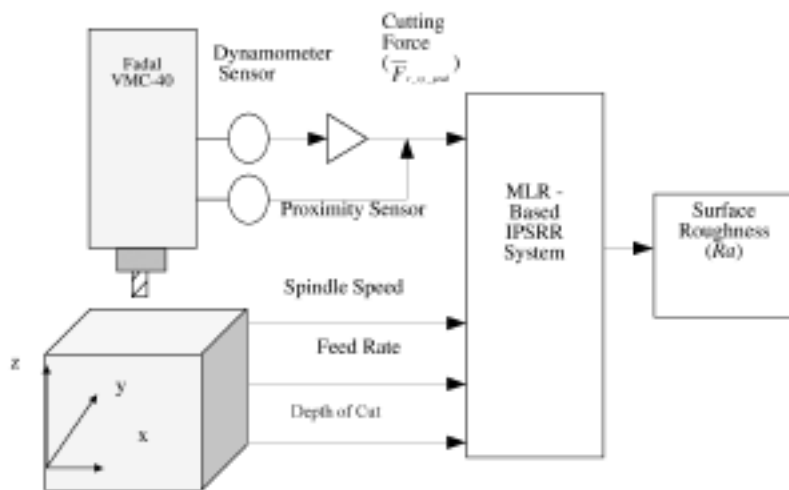
rpm), and three levels of depth of cut (0.04, 0.06, and 0.08 in.), was designed for the experiments with two replicates of each experiment. Two end milling tools (1/2 in. with four teeth) were used to cut the workpiece. Therefore, a total of $8 \times 4 \times 3 \times 2 \times 2 = 384$ sets of training data were collected. Cutting forces (F_x , F_y , and F_z) were collected using a dynamometer, as shown in Figure 1. The average resultant force of the x and y directions ($\bar{F}_{r_{xy}}$), average resultant peak force ($\bar{F}_{r_{xy_peak}}$), average cutting force of the z direction (\bar{F}_z), and average resultant force of the x , y , and z directions ($\bar{F}_{r_{xyz}}$) were calculated using Equations 2, 3, 4, and 5.

The 384 specimens were measured offline with a Pocket Surf stylus type profilometer (produced by Federal Products Co.) to obtain surface roughness (R_a) in this study. A JMP (a product of the SAS Institute) statistical software package was used to calculate the correlation coefficient between surface roughness and cutting forces. The results were $\rho_{Ra-\bar{F}_{r_{xy}}} = 0.49$, $\rho_{Ra-\bar{F}_{r_{xy_peak}}} = 0.53$, $\rho_{Ra-\bar{F}_z} = 0.46$, and $\rho_{Ra-\bar{F}_{r_{xyz}}} = 0.43$; therefore, the average resultant peak force of the x and y directions ($\bar{F}_{r_{xy_peak}}$) had the highest correlation coefficient with surface roughness and was selected as the input parameter for the MLR-IPSRR system.

The Proposed MLR-IPSRR System

After the most significant force was identified, the MLR-IPSRR system shown in Figure 4 was proposed. From Figure 4, one can see the

Figure 4. The structure of the proposed MRL-IPSRR system.



input parameters (average resultant peak force [$\bar{F}_{r_{xy_peak}}$], spindle speed [S], feed rate [F], and depth of cut [D]) and the output parameter (surface roughness [Ra]) used to generate the MLR-IPSRR system. The proposed MLR-IPSRR system is given as:

$$\begin{aligned} Ra_i = & \beta_0 + \beta_1 F_i + \beta_2 S_i + \beta_3 D_i + \beta_4 \bar{F}_{r_{xy_peak}} \\ & + \beta_{12} F_i * S_i + \beta_{13} F_i * D_i + \beta_{14} F_i * \bar{F}_{r_{xy_peak}} \\ & + \beta_{23} S_i * D_i + \beta_{24} S_i * \bar{F}_{r_{xy_peak}} \\ & + \beta_{34} D_i * \bar{F}_{r_{xy_peak}} + \beta_{123} F_i * S_i * D_i \\ & + \beta_{124} F_i * S_i * \bar{F}_{r_{xy_peak}} + \beta_{234} S_i * D_i * \bar{F}_{r_{xy_peak}} \\ & + \beta_{1234} F_i * S_i * D_i * \bar{F}_{r_{xy_peak}} + \varepsilon_i \end{aligned}$$

where β are coefficients of the regression model, Ra_i is the surface roughness, F_i is the feed rate, S_i is the spindle speed, D_i is the depth of cut, $\bar{F}_{r_{xy_peak}}$ is the average resultant peak force of the x and y directions, and $\varepsilon_i \sim N(0, \sigma^2)$, where i is the number of data sets. To obtain data for the development of a multiple regression prediction model, a total of 384 experimental runs have taken place using the cutting combination indicated in the experimental design section.

Therefore, in this study, $i = 1, 2, 3, \dots, 384$.

Analysis and Results of the System

After utilizing the JMP software package, the results of the surface roughness MLR model were generated as follows:

$$\begin{aligned} Ra_{predicted} = & 57.066 - 0.024 * S + 4.142 * F - \\ & 0.001 * (S - 2125) * (F - 13) + 491.056 * D + \\ & 0.630 * (S - 2125) * (D - 0.06) + 41.820 * (F - \\ & 13) * (D - 0.06) - 0.351 * \bar{F}_{r_{xy_peak}} - 0.0007 * \\ & (S - 2125) * (\bar{F}_{r_{xy_peak}} - 75.787) + 0.015 * \\ & (F - 13) * (\bar{F}_{r_{xy_peak}} - 75.787) - 0.326 * \\ & (D - 0.06) * (\bar{F}_{r_{xy_peak}} - 5.787) + 0.099 * \\ & (S - 2125) * (F - 13) * (D - 0.06) - 0.0001 * (S - \\ & 2125) * (F - 13) * (\bar{F}_{r_{xy_peak}} - 75.787) + 0.01 * \\ & (S - 2125) * (D - 0.06) * (\bar{F}_{r_{xy_peak}} - 5.787) + \\ & 0.722 * (F - 13) * (D - 0.06) * (\bar{F}_{r_{xy_peak}} - 75.787) \\ & - 0.0016 * (S - 2125) * (F - 13) * (D - 0.06) * \\ & (-\bar{F}_{r_{xy_peak}} 75.787) \end{aligned}$$

The effect of tests showed that the feed rate, spindle speed, average resultant peak force, and depth of cut influenced the surface roughness significantly since the p values of each main effect (feed rate, spindle speed, average resultant peak force, and depth of cut) were less than a =

0.01 significant level). That is, the surface roughness was mainly determined by the feed rate, spindle speed, average resultant peak force, and depth of cut in end milling operations. The MLR model was also significant with the p value less than $a = 0.01$. Therefore, the MLR model can be effectively used in this research.

Once the MLR model had been established, the MLR recognition model was tested using 20 sets of cutting conditions that were different from the cutting conditions of experimental designs. The MLR-IPSRR model was implemented in the prediction of the surface roughness while the machining process was taking place. The results of the predicted surface roughness (Ra_i^{MLR}) were compared with the finished parts (Ra_{i-m}) that were measured by using a Pocket Surf portable surface roughness gauge. Then, the individual precision Φ_i^{MLR} of each experimental run (i) was evaluated based on the following equations.

$$\Phi_i^{MLR} = 1 - \frac{|Ra_i^{MLR} - Ra_{i-m}|}{Ra_i} \quad (8)$$

$$\bar{\Phi}^{MLR} = \frac{\sum_{i=1}^{20} \Phi_i^{MLR}}{20} \quad (9)$$

where Φ_i^{MLR} is the precision of i th testing run, and $\bar{\Phi}^{MLR}$ is the average precision of the 20 testing data, $i = 1 \dots 20$.

The results showed that the capability of the surface roughness prediction was about 86% for the testing experimental data in this study. Therefore, one can see that the surface roughness (Ra) can be predicted effectively by the above-mentioned MLR-IPSRR system.

What We Learned

The purpose of this study was to analyze cutting forces to find out the most significant cutting force magnitude that affected surface roughness and to evaluate whether a MLR approach for surface roughness recognition could be used for prediction in the IPSRR system. Our main conclusions are summarized as follows:

- The average resultant peak force ($\bar{F}_{r_{xy_peak}}$) was identified to be the most significant force to affect surface roughness in this study.

- Spindle speed, feed rate, average peak cutting force, and depth of cut are significant in affecting surface roughness in end milling operations and the determination of the coefficient is R^2 of 0.62 in the MLR model.
- The MLR-IPSRR system is approximately 86% accurate in predicting surface roughness while the machining process is taking place.

This research assumed that the CNC milling machine was effective and stable to conduct all experiments under each cutting condition using an HSS end mill to cut 6061 aluminum material. We believe that the proposed IPSRR system could eventually be implemented in the new age of CNC machines. This would be more likely if additional research and testing could be done such as (a) including different

tool material, tool radius, workpiece material, and lubricants in the system and (b) using different methodologies, such as fuzzy logic, neural networks, and fuzzy nets, to provide the IPSRR system with a learning capability. With this capability, the system could be adopted to different machines produced from different CNC manufacturers.

Dr. Lieh-Dai (John) Yang is an associate professor in the Department of Industrial Management at Nan-Kai College, Nantou, Taiwan.

Dr. Joseph Chen is a professor in the Department of Industrial Education and Technology at Iowa State University. He is a member of Alpha Xi Chapter of Epsilon Pi Tau.

References

- Chen, J. C., & Lou, M. S. (2000). Fuzzy-nets based approach to using an accelerometer for an in-process surface roughness prediction system in milling operations. *International Journal of Computer Integrated Manufacturing*, 13(4), 358-368.
- Chen, J. C., & Lou, S-J. (1999). Statistical and fuzzy-logic approaches in on-line surface roughness recognition system for end-milling operations. *International Journal of Flexible Automation and Integrated Manufacturing*, 6(1&2), 53-78.
- Chen, J. C., & Savage, M. (2001). A fuzzy-net-based multiple in-process surface roughness recognition system in milling operations. *International Journal of Advanced Manufacturing Technology*, 17, 670-676.
- Coker, S. A., & Shin, Y. C. (1996). In-process control of surface roughness due to tool wear using a new ultrasonic system. *International Journal of Machine Tools & Manufacture*, 36(3), 411-422.
- Degarmo, E. P., Black, J. T., & Kohser, R. A. (1999). *Material processes in manufacturing*. Upper Saddle River, NJ: Prentice Hall.
- Fuh, K-H., & Wu, C-F. (1995). A proposed statistical model for surface quality prediction in end-milling of Al alloy. *International Journal of Machine Tools & Manufacture*, 35(8), 1187-1200.
- Jang, D-Y., Choi, Y-G., Kim, H-G., & Hsiao, A. (1996). Study of the correlation between surface roughness and cutting vibrations to develop an on-line roughness measuring technique in hard turning. *International Journal of Machine Tools & Manufacture*, 36(4), 453-464.
- Lee, T. S., & Lin, Y. J. (2000). A 3D predictive cutting force model for end milling of parts having sculptured surfaces. *International Journal of Advanced Manufacturing Technology*, 16, 773-783.
- Montgomery, D. C. (1997). *Design and analysis of experiments*. New York: Wiley.
- Susic, E., & Grabec, I. (1995). Application of a neural network to the estimation of surface roughness from AE signals generated by friction process. *International Journal of Machine Tools & Manufacture*, 35(8), 1077-1086.
- Tsai, Y., Chen, J. C., & Lou, S. (1999). An in-process surface recognition system based on neural networks in end milling cutting operations. *International Journal of Machine Tools & Manufacture*, 39, 583-605.

